

RESEARCH ARTICLE | JANUARY 29 2016

Electron energy distribution functions and fractional power transfer in “cold” and excited CO₂ discharge and post discharge conditions

L. D. Pietanza; G. Colonna; G. D'Ammando; ... et. al



Physics of Plasmas 23, 013515 (2016)

<https://doi.org/10.1063/1.4940782>



CrossMark

Articles You May Be Interested In

Superelastic collisions under low temperature plasma and afterglow conditions: A golden rule to estimate their quantitative effects

Physics of Plasmas (March 2015)

Time-dependent Boltzmann equation in a self-sustained discharge XeCl laser: Influence of electron-electron and superelastic collisions

Journal of Applied Physics (January 1990)

Self-consistent electron energy distribution functions, vibrational distributions, electronic excited state kinetics in reacting microwave CO₂ plasma: An advanced model

Physics of Plasmas (February 2020)

Electron energy distribution functions and fractional power transfer in “cold” and excited CO₂ discharge and post discharge conditions

L. D. Pietanza,^{a)} G. Colonna, G. D’Ammando, A. Laricchiuta, and M. Capitelli
Nanotec-CNR, sect. Bari, via Amendola 122/D, 70126 Bari, Italy

(Received 30 October 2015; accepted 12 January 2016; published online 29 January 2016)

A Boltzmann equation, in the presence of superelastic vibrational and electronic collisions and of electron–electron Coulomb collisions, has been solved in CO₂ plasma in discharge and post discharge conditions. Superelastic vibrational collisions play an important role in affecting the electron energy distribution function (eedf) in a wide range of the reduced electric field E/N and of vibrational temperatures characterizing the vibrational modes of CO₂. An important result is the dependence of fractional power losses and of the relevant rate coefficients on the vibrational temperatures of the system. Superelastic electronic collisions, on the other hand, are the main processes affecting eedf and related quantities in the post discharge conditions (i.e., $E/N = 0$). In particular at low vibrational temperatures, the superelastic electronic collisions form an important plateau in the eedf, largely influencing the rate coefficients and the fractional power transfer. © 2016 AIP Publishing LLC.
[\[http://dx.doi.org/10.1063/1.4940782\]](http://dx.doi.org/10.1063/1.4940782)

I. INTRODUCTION

Large attention has been devoted in the past to the characterization of electron energy distribution function (eedf) in He/CO₂/CO/N₂ plasmas for the optimization of infrared CO₂ lasers.^{1–3} Less attention, on the contrary, is being devoted to the characterization of eedf in pure CO₂ plasmas, which are presently used for the activation of CO₂ molecules for different energy applications^{4–7} with particular attention to the reforming of CH₄-CO₂ mixtures by cold plasma technology.⁸ In the different conditions, non equilibrium vibrational excitation and de-excitation processes take a paramount importance in affecting eedf and related quantities. In particular, superelastic vibrational collisions are expected to strongly modify the tail of eedf, increasing, by orders of magnitude, the high threshold energy electron impact excitation (including dissociation) and ionization rates and, at the same time, the fractional power transfer into the different CO₂ degrees of freedom. This latter quantity was widely used by infrared laser physics researchers to understand the best E/N value to be used for optimizing the laser output. The dependence of the fractional power losses in the different channels is univocally determined as a function of average electron energy (i.e., for the cold gas approximation), following the pioneering work of Nighan,⁹ without allowing their dependence on the presence of excited states as well as of the ionization degree (ID). In the present paper, we will show that their influence is as more important as higher are the relevant vibrational temperatures and the ionization degree, taking also an important role in the post discharge conditions. In these last conditions, superelastic electronic collisions form important plateau(x) in eedf with large consequences on the relevant rates and fractional power channels.

These considerations are strictly linked to the possibility to construct tables of rates as a function of average electron

energy (i.e., as a function of E/N), an approximation widely used in the global models. The presence of excited states strongly modifies eedf especially at low E/N values so that the rates do not only depend on the E/N value but also on the concentration of excited states as well as on the ionization degree.

The dependence of fractional power losses on the concentration of excited states as well as the non-uniqueness of rate coefficient values as a function of average electron energy will be discussed in the present paper.

In general, in pure CO₂ plasmas, the eedf and the derived rates largely depend on the number of e-V processes inserted in the Boltzmann equation. The results reported in the bulk of the present paper have been obtained by solving the Boltzmann equation by considering the e-V processes reported in the Hake and Phelps database.¹⁰ A more adequate model should include all e-V transitions linking the vibrational ladder corresponding to the asymmetric mode of CO₂. The corresponding cross sections can be evaluated on the basis of the scaling equation of Fridman and Kennedy,¹¹ as recently used by Kozak and Bogaerts.⁴ The insertion of new cross sections directly affects eedf and indirectly the relevant dissociation and ionization rates.

The present paper is divided into 7 sections. After the introduction, Section II presents the Boltzmann equation for the electron energy distribution function (eedf) and its dependence on superelastic vibrational and electronic collisions. In the same section, we discuss the dependence of fractional power losses in the cold gas approximation as compared with situations with increasing concentrations of excited states. In Section III, we report the non univocal dependence of rate coefficients on average electron energy under different non-equilibrium conditions, a topic important for assessing the accuracy of global models. Section IV considers eedf in the post discharge conditions.

Section V reports the dependence of eedf on the insertion in the Boltzmann solver of a complete set of e-V cross

^{a)}E-mail: luciadaniela.pietanza@cnr.it

sections linking the asymmetric mode. Finally, conclusions and perspectives are reported in Section VI.

II. THE BOLTZMANN EQUATION: THE ELECTRON ENERGY DISTRIBUTION FUNCTIONS AND THE FRACTIONAL POWER TRANSFER

As anticipated, we solve an appropriate Boltzmann equation written in compact form as^{12–19}

$$\frac{dn(\varepsilon, t)}{dt} = -\frac{dJ_E}{d\varepsilon} - \frac{dJ_{el}}{d\varepsilon} - \frac{dJ_{e-e}}{d\varepsilon} + S_{in} + S_{sup}, \quad (2.1)$$

where $n(\varepsilon, t)d\varepsilon$ represents the number of electrons in the energy range ε and $\varepsilon + d\varepsilon$. The different terms on the right hand side of Eq. (2.1) represent the flux of electrons along the energy axis, respectively, due to the electric field $\frac{dJ_E}{d\varepsilon}$, elastic electron-molecule collisions $\frac{dJ_{el}}{d\varepsilon}$, electron-electron (e-e) collisions $\frac{dJ_{e-e}}{d\varepsilon}$, and inelastic S_{in} and superelastic S_{sup} collisions. Explicit expressions of the different contributions, including the electron-electron one, can be found in Refs. 15, 18, and 19. Eq. (2.1) derives from the work of Rockwood¹³ and it is based on a two term Boltzmann expansion, which is considered adequate against the more accurate multiterm approach²⁰ in the context of the present application, especially considering the present knowledge of the relevant cross sections.

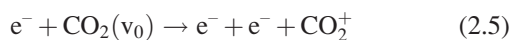
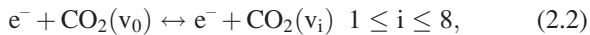
A simplified CO₂ energy ladder is considered describing the interaction of electrons with:

- (1) eight vibrational levels (v_i with $0 \leq i \leq 8$), the fundamental v_0 (000), the first bending mode level v_1 (010), the first asymmetric mode level v_8 (001), and five mixing levels (Fermi resonance levels) v_2 - v_7 ($0n0 + n00$);
- (2) two electronic levels (e_1, e_2) with threshold energies, respectively, at 7.0 and 10.5 eV, the first one considered as a dissociative channel and the second as an excitation one.

The relevant cross sections have been taken from the database of Hake and Phelps.¹⁰

In such database, the 10.5 eV electronic state is stable, contrary to Itikawa database.²¹ In any case, we believe that in the CO₂ system, including also the CO system (not considered in the present paper) coming from the dissociation process, stable electronic states at about 10.5 eV can exist.

Briefly, the Hake and Phelps database considers the following processes:



corresponding to the electron impact vibrational excitation/de-excitation from ground level v_0 towards selected upper vibrational levels v_i (Eq. (2.2)), the electronic excitation from ground level v_0 towards e_2 (Eq. (2.3)), the dissociation (Eq. (2.4)) and the ionization (Eq. (2.5)) process from ground level v_0 .

The different thresholds of the processes are reported in Table I, the first process referring to momentum transfer.

It should be noted that the vibrational ladder(s) used in this work follows the ideas developed in the past for the characterization of IR CO₂ laser. More complicated CO₂ vibrational energy ladders have been developed, recently, by Armenise and Kustova²² for the study of CO₂ non-equilibrium vibrational kinetics in the hypersonic boundary layer of reentering bodies in the Mars atmosphere in dissociation-recombination regime. Their vibrational ladders contain thousand and thousand levels and their use in plasma applications is, at the moment, very complicated due to the lack of electron-molecule cross sections linking the vibrational ladder.

A time dependent Boltzmann solver is used taking the reduced electric field E/N , the vibrational temperatures of the different modes, and the ID as free parameters. In particular, two vibrational temperatures are considered: T_1 describing levels v_1 - v_7 and T_2 the asymmetric mode level v_8 . Moreover, superelastic collisions with the electronic state at 10.5 eV are considered either in discharge and post discharge conditions. Under discharge conditions, we select a concentration of the electronic state from a Boltzmann distribution at the same T_2 temperature as the asymmetric mode level v_8 , while in the post discharge conditions, we assume a fixed concentration of 10^{-4} , estimated following the considerations of Pietanza *et al.*¹²

The choice of parameters ($E/N, T_1, T_2$) has been made by trying to reproduce the average energies found under experimental conditions (electron average energy in the range 1–4 eV, see Kozak *et al.*^{4,5} and Silva *et al.*⁶). The choice of T_2 is in line with the estimation made in the experiments of Silva *et al.*⁶ (see Fig. 11 and comments). On the other hand, we consider $T_1 < T_2$ and this comes from experiments on the CO₂ laser²³ and is justified by the small values of VT rates in the asymmetric mode as compared with the corresponding rates in the other modes.

The ionization degree value used (10^{-3}), in both discharge and post discharge conditions, must be considered, in any case, as an upper limit. Cold plasmas are usually characterized by an ionization degree lower than the reported 10^{-3} one. The results qualitatively suggest that ionization degrees

TABLE I. Electron impact energy exchange processes considered in the Boltzmann equation for pure CO₂.

| Notation | State | Energy (eV) |
|------------------------------|---------------|-------------|
| CO ₂ (v_0) | (000) | 0.000 |
| CO ₂ (v_1) | (010) | 0.083 |
| CO ₂ (v_2) | (020) + (100) | 0.167 |
| CO ₂ (v_3) | (030) + (110) | 0.252 |
| CO ₂ (v_4) | (0n0) + (n00) | 0.339 |
| CO ₂ (v_5) | (0n0) + (n00) | 0.442 |
| CO ₂ (v_6) | (0n0) + (n00) | 0.505 |
| CO ₂ (v_7) | (0n0) + (n00) | 2.500 |
| CO ₂ (v_8) | (001) | 0.291 |
| CO ₂ (e_1) | | 7.000 |
| CO ₂ (e_2) | | 10.500 |
| CO ₂ ⁺ | | 13.300 |

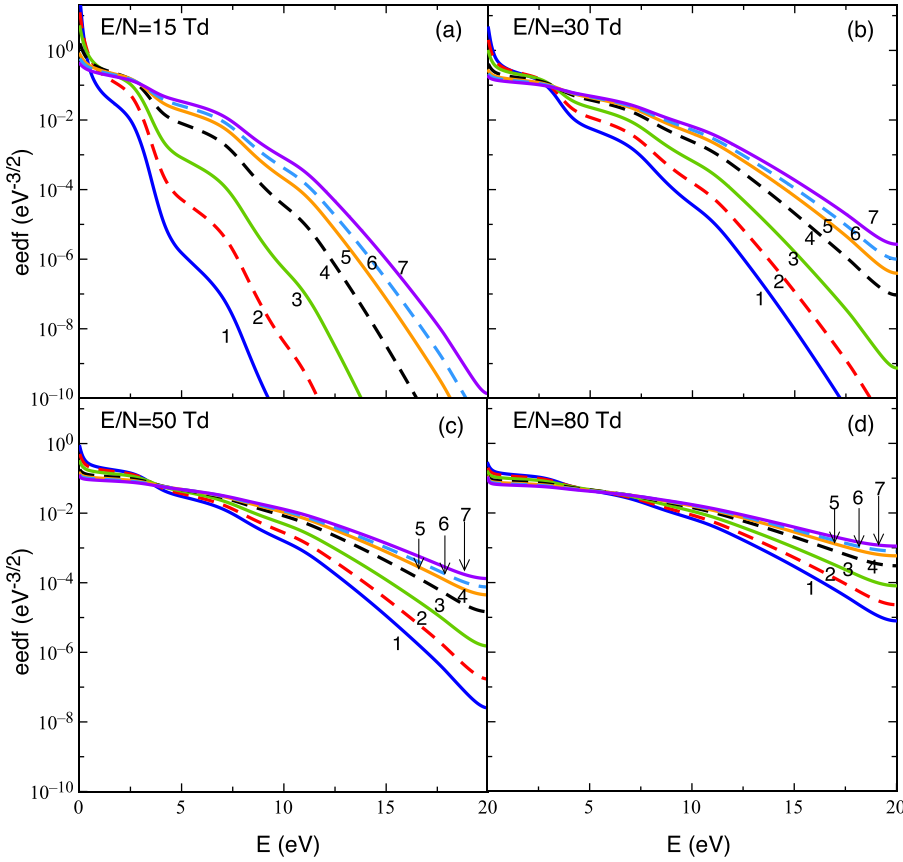


FIG. 1. (a)–(d). Electron energy distribution function versus electron energy at different reduced electric field values (a) 15 Td, (b) 30 Td, (c) 50 Td, and (d) 80 Td for different couples of (T_1 - T_2) vibrational temperatures (see Table II), neglecting e-e collisions.

$<10^{-3}$, while keeping their influence on the electron energy distribution function in the post discharge, lose their role under discharge conditions.

Figs. 1(a)–1(d) report the eedf behavior as a function of electron energy at fixed E/N (15, 30, 50 and 80 Td) for different couples of T_1 , T_2 values (see Table II), without including e-e collisions.

For $T_1 = T_2 = 0$ K, i.e., in the cold gas approximation, only elastic and inelastic (including dissociation and ionization) collisions from ground vibrational state affect the eedf, while superelastic vibrational and electronic collisions give their contribution on eedf only for T_1 and $T_2 > 0$. The effect of superelastic vibrational collisions results in an enlargement of eedf, which follows the increase of the absolute values of T_1 and T_2 temperatures, this effect decreasing with the increase of E/N . The results reported in Figs. 1(a)–1(d), which have been obtained without taking into account e-e Coulomb collisions, indicate a large deviation of eedf from

the Maxwell behavior, showing characteristic structures due to superelastic vibrational collisions. These structures appear smoothed in the results reported in Figs. 2(a)–2(d), which have been calculated by including e-e collisions with an ionization degree of 10^{-3} .

Figs. 3(a)–3(d) report the fractional power losses dissipated in the different channels as a function of E/N for different (T_1 - T_2) couple values of Table II.

These fractional power losses have been calculated as the ratio between the electron energy transferred per unit time and volume from electrons to different CO_2 excitation channels, vibrational (Q_{vib}), dissociative (Q_{diss}), electronic (Q_{electr}), and ionization (Q_{ion}), and the electron energy per unit time and volume gained by the electrons from the electric field (Q_E).

In particular, if we consider, as an example, the vibrational energy channel, the energy transferred into the vibrational excitation per unit time and volume can be written as

$$Q_{\text{vib}} = N_e N_{\text{tot}} (A - B), \quad (2.6)$$

$$A = \sum_{v_i} \sum_{v_j} \chi_{\text{CO}_2}(v_i) K_d(v_i, v_j) \epsilon_{v_i, v_j}^*, \quad (2.7)$$

$$B = \sum_{v_i} \sum_{v_j} \chi_{\text{CO}_2}(v_j) K_r(v_j, v_i) \epsilon_{v_i, v_j}^*, \quad (2.8)$$

where N_e , N_{tot} are the electron and total density, $\chi_{\text{CO}_2}(v_i)$ and $\chi_{\text{CO}_2}(v_j)$ the molar fractions of CO_2 into the vibrational levels v_i and v_j (with $v_i < v_j$), $K_d(v_i, v_j)$ and $K_r(v_j, v_i)$ the electron impact vibrational excitation and de-excitation rate

TABLE II. T_1 and T_2 vibrational temperature couples used in the test cases.

| Test cases | T_1 (K) | T_2 (K) |
|------------|-----------|-----------|
| 1 | 0 | 0 |
| 2 | 500 | 1500 |
| 3 | 1000 | 2000 |
| 4 | 2000 | 3000 |
| 5 | 3000 | 5000 |
| 6 | 4000 | 6000 |
| 7 | 6000 | 8000 |

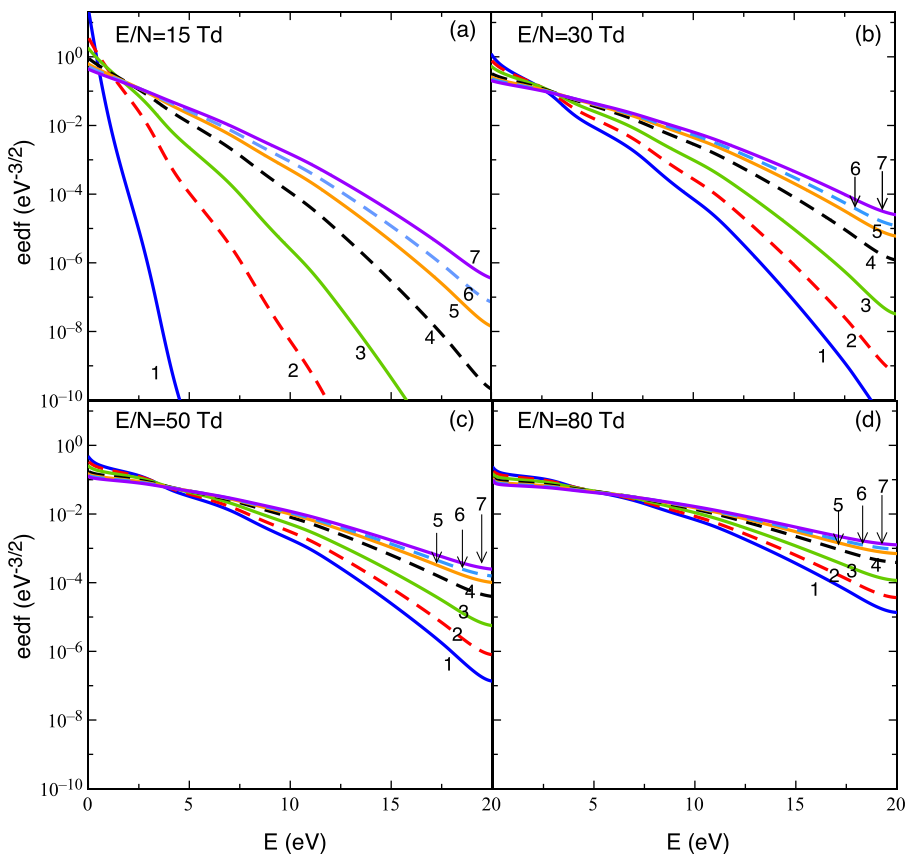


FIG. 2. (a)–(d). Electron energy distribution function versus electron field energy at different reduced electric field values (a) 15 Td, (b) 30 Td, (c) 50 Td, and (d) 80 Td for different couples of (T_1-T_2) vibrational temperatures (see Table II), including e-e collisions (ionization degree (ID) of 10^{-3}).

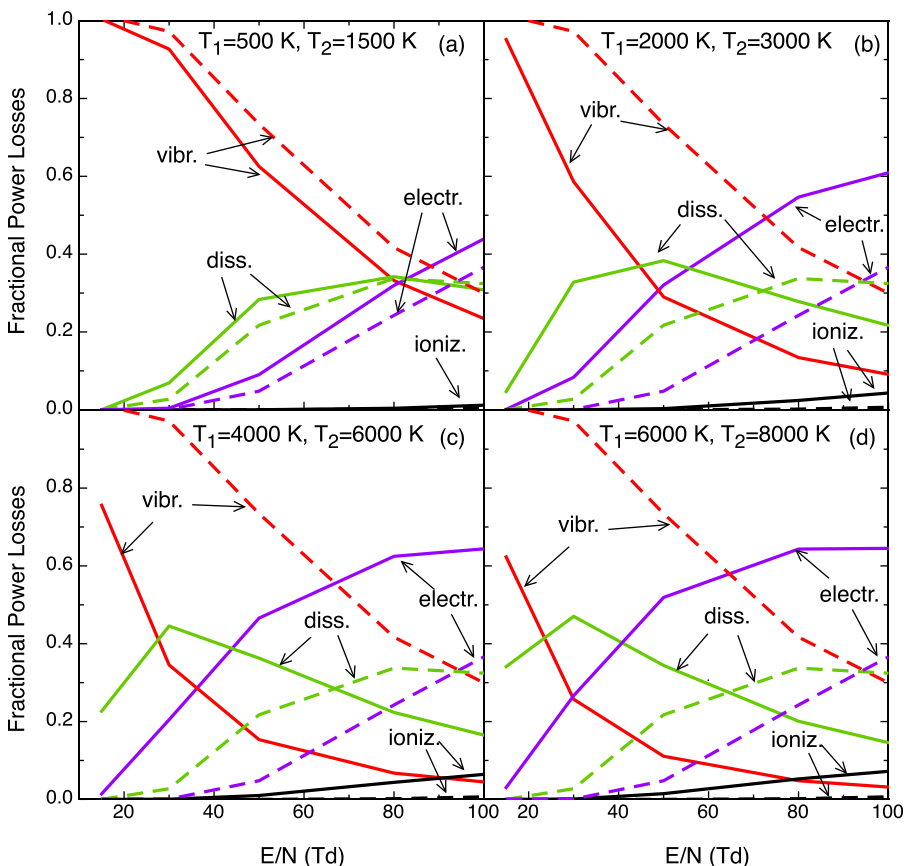


FIG. 3. (a)–(d). Electron fractional power losses dissipated in the different channels (vibrational, dissociative, electronic excitation, and ionization) as a function of the reduced electric field E/N for different couples of (T_1-T_2) vibrational temperatures (see Table II), (a) $T_1=500$ K, $T_2=1500$ K (case 2); (b) $T_1=2000$ K, $T_2=3000$ K (case 4); (c) $T_1=4000$ K, $T_2=6000$ K (case 6); and (d) $T_1=6000$ K, $T_2=8000$ K (case 7), with (full lines) and without (dashed lines) superelastic collisions.

coefficients, and ε_{v_i, v_j}^* the threshold energy. The electron energy per unit time and volume gained from the electric field is, instead, given by

$$Q_E = N_e v_d q_e E, \quad (2.9)$$

where v_d is the drift velocity, q_e the electron charge, and E the electric field strength. The results shown in Fig. 3 confirm the literature results^{6,7,9,24} for the cold gas approximation, i.e., the major portion of the discharge power is transferred from plasma electrons to vibrational excitation of CO₂ molecules in a wide range of E/N . The dissociative, the electronic excitation, and the ionization channels are activated by increasing the reduced electric field value. In particular, dissociation and excitation channels become equal to the vibrational one only at 90 Td, thus suggesting that other dissociative mechanisms should exist at low E/N values.^{5,7,9} Moreover, inspection of the results in Fig. 3 shows the importance of excited states and superelastic collisions in affecting the energy transfer rates. In particular, the superelastic vibrational collisions reduce the power losses in the vibrational channel and consequently modify the power losses in the other channels. It is clear that superelastic collisions, by pumping electrons at higher energy, promote dissociative and electronic excitation energy channels, whose rates depend strongly on the eedf tail. These plots can be indeed taken as indicators of the importance of vibrational excitation in the different processes, clearly warning on the use of these plots in the cold gas approximation. The results reported in Figs. 3(a)–3(d) have been obtained without considering e-e collisions in the Boltzmann equation. Inclusion of these collisions, at an ionization degree of 10^{-3} , changes the reported results, especially at higher vibrational temperatures, as it can be appreciated in Figs. 4(a) and 4(b). In this figure, fractional power losses with and without e-e collisions are reported at two different couples of (T_1 - T_2) temperatures (Table II), omitting the results in the cold gas approximation.

III. THE DEPENDENCE OF ELECTRON IMPACT RATES ON THE NON-EQUILIBRIUM PLASMA CONDITIONS

The results presented in this section can be used to estimate the accuracy of global approaches in plasma chemistry applications. Global models tend to simplify the relevant kinetics defining different temperatures to which calculate the rates. In particular, a macroscopic equation for the electron temperature (T_e) is derived taking into account electron energy losses and gains. Then, two approaches are possible: on one hand, this electron temperature can be used to calculate the electron molecule rates by assuming, for electrons, a Maxwell distribution function; on the other hand, one can use a Boltzmann solver to calculate the rate coefficients at a given E/N , which reproduces the average electron energy from the macroscopic energy equation.⁴ In the cold gas approximation, strong deviations are observed between the eedfs calculated by a Maxwell distribution at T_e and the corresponding ones calculated from a Boltzmann solver at E/N characterized by the same electron temperature, for nitrogen.^{25,26} In this section, we would like to verify these assumptions commonly used in global model in the case of CO₂ plasma.

Figs. 5(a)–5(d) report electron impact rates of the processes (2.2) (limited to the asymmetric excitation), (2.3), (2.4), and (2.5) as a function of the average electron energy. Figs. 5(a)–5(d) show just a sample of all the collected rate data obtained from calculations in post discharge and discharge conditions, by varying the values of the reduced electric field ($E/N = 15$ –30–50–80–100 Td), the ionization degree (10^{-5} – 10^{-3}), the presence or not of e-e collisions, and the different vibrational temperatures (reported in Table II). The most important result of this figure is that at fixed average energy (especially for energy less than 2.5 eV), the rates depend on the non equilibrium plasma conditions, a point which should be taken into account in the global models.

In particular, only the rates of low threshold energy processes, such as the vibrational excitation (000)→(001)

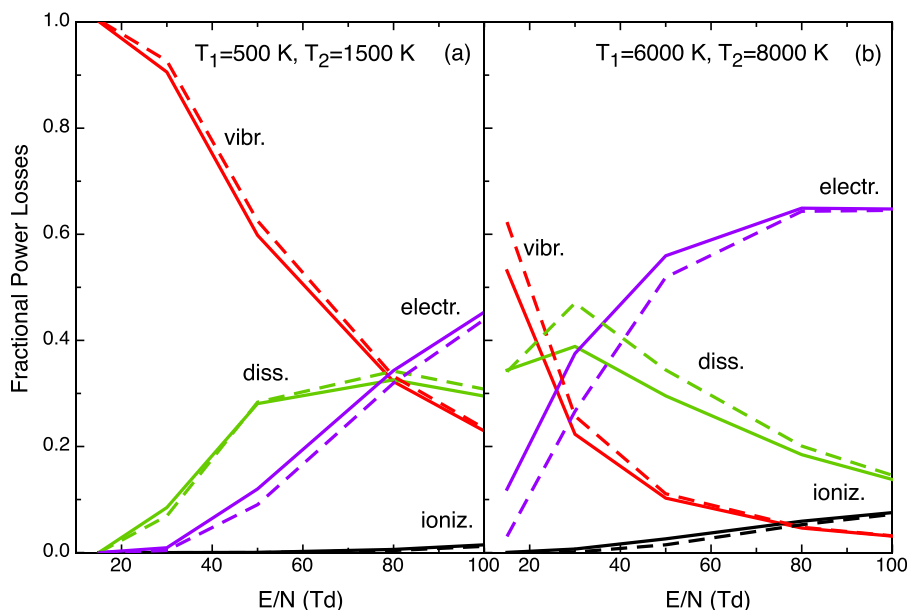


FIG. 4. (a) and (b). Electron fractional power losses dissipated in the different channels (vibrational, dissociative, electronic excitation, and ionization) as a function of the reduced electric field E/N for (a) $T_1 = 500$ K, $T_2 = 1500$ K (case 2 of Table II) and (b) $T_1 = 6000$ K, $T_2 = 8000$ K (case 7 of Table II), including (full lines) and neglecting (dashed lines) e-e collisions (ionization degree of 10^{-3}).

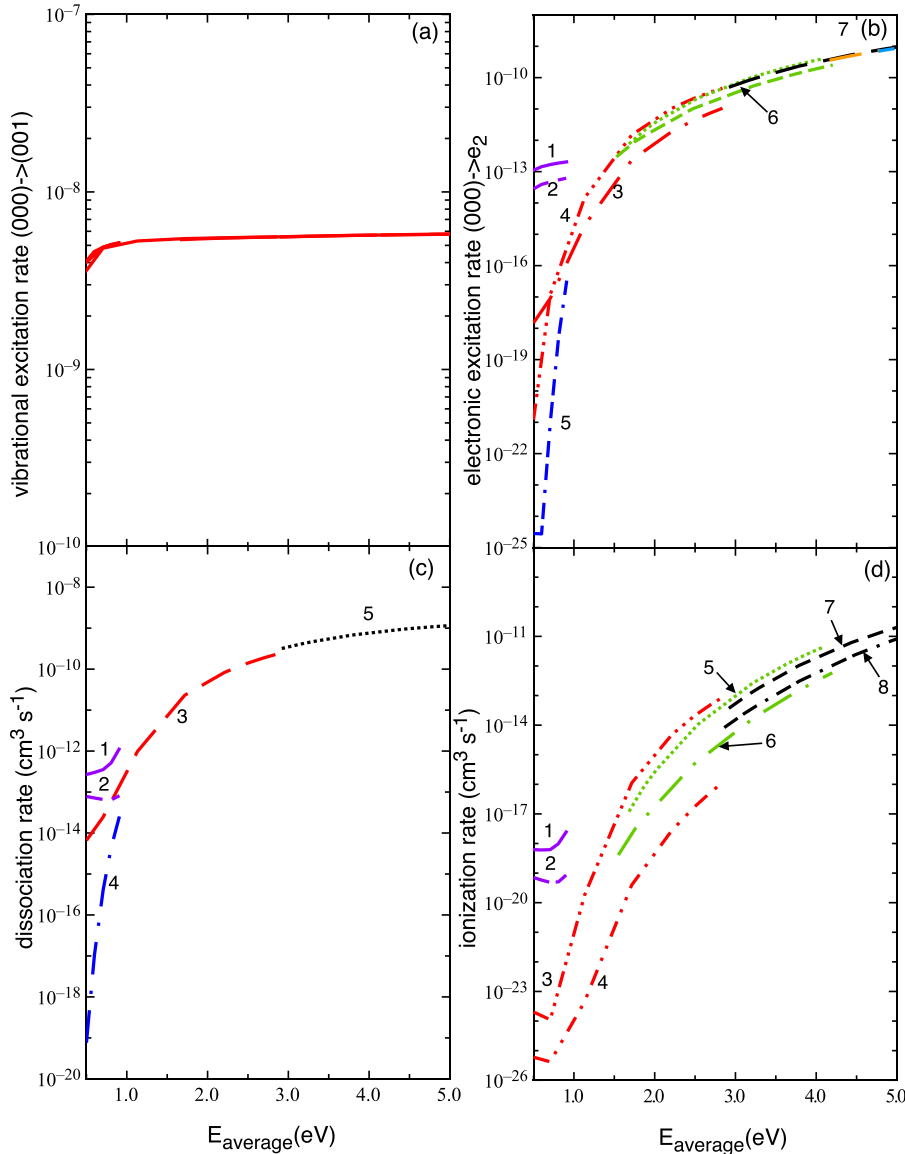


FIG. 5. (a)–(d) Rate coefficients of (a) vibrational excitation $(000) \rightarrow (001)$, (b) electronic excitation $(000) \rightarrow \text{CO}_2(e_2)$, (c) dissociation, and (d) ionization as a function of the electron average energy. The data derive from calculations in post discharge conditions (PDS) and in discharge conditions (DS) at different E/N values, different ID, with or without ee collisions and with different vibrational temperature, reported in Table II. The different curves correspond to the following conditions: (b) 1: (PDS, $E/N=0$ Td, $ID=10^{-3}$, with ee); 2: (PDS, $E/N=0$ Td, without ee); 3: (DS, $E/N=15$ Td, without ee); 4: (DS, $E/N=15$ Td, $ID=10^{-3}$, with ee); 5: (DS, $E/N=0$ Td, without ee); 6: (DS, $E/N=30$ Td, without ee); 7: (DS, $E/N=50$ Td, $E/N=80$ Td, $E/N=100$ Td, with and without ee); (c) 1: (PDS, $E/N=0$ Td, $ID=10^{-3}$, with ee); 2: (PDS, $E/N=0$ Td, without ee); 3: (DS, $E/N=15$ Td, without ee); 4: (DS, $E/N=0$ Td, $ID=10^{-5}$, with ee); 5: (DS, $E/N=50$ Td, $ID=10^{-3}$, with ee); and (d) 1: (PDS, $E/N=0$ Td, $ID=10^{-3}$, with ee); 2: (PDS, $E/N=0$ Td, without ee); 3: (DS, $E/N=15$ Td, $ID=10^{-3}$, with ee); 4: (DS, $E/N=15$ Td, without ee); 5: (DS, $E/N=30$ Td, $ID=10^{-3}$, with ee); 6: (DS, $E/N=30$ Td, $ID=10^{-5}$, with ee); 7: (DS, $E/N=50$ Td, $ID=10^{-3}$, with ee); 8: (DS, $E/N=50$ Td, without ee).

(see Fig. 5(a)), are a function of actual average electron energy calculated by the Boltzmann solver. On the contrary, the rates of high threshold energy processes (such as electronic excitation (Fig. 5(b)), dissociation (Fig. 5(c)) and ionization (Fig. 5(d))) do not have a univocal correspondence with average electron energy, since they depend also on the ee df shape in the high energy part and thus on plasma conditions.

Global models, which use look up tables to obtain electron impact rate values from average electron energy, obtained either imposing Maxwell distribution functions or by using a Boltzmann solver for ee df in the cold gas approximation, cannot give a reliable rate estimation. This can happen in particular, in the CO_2 cold plasmas, which should operate at low electron average energies to maximize the role of vibrational energy in the process. Global models can be in general used only at large values of the reduced electric field.

In the same figure, we have also reported the behavior of the rates in the post-discharge conditions (which presents a peculiar trend), following the corresponding behavior of ee df reported in Section V.

IV. POST DISCHARGE CONDITIONS

Let us now consider the post discharge conditions, i.e., $E/N=0$. In this case, we have supposed that, at the end of the electrical discharge, soon before the starting of the post discharge, we have different vibrational distributions characterized by their own vibrational temperatures and by a fixed molar concentration of the 10.5 eV electronic excited state ($\text{CO}_2(e_2)$) of 10^{-4} . The last concentration, in combination with low vibrational temperatures, can be obtained by considering atmospheric nanosecond pulsed discharge with an electron density of 10^{14} – 10^{15} cm^{-3} . On the other hand, the higher vibrational temperatures conditions can be obtained by continuous atmospheric discharges with residence times of the order of 10^{-2} s, electron density of 10^{11} cm^{-3} , and an e -V rate of 10^{-9} cm^3/s . In this case, the typical relaxation time $(n_e k_{eV})^{-1}$ is of the order of the considered residence time so that we can expect large concentrations of vibrationally excited states.

Figs. 6(a) and 6(b) report the trend of the stationary ee df in this regime, by inserting and neglecting e - e collisions. The peak at 10.5 eV is due to the superelastic electronic collisions of the kind

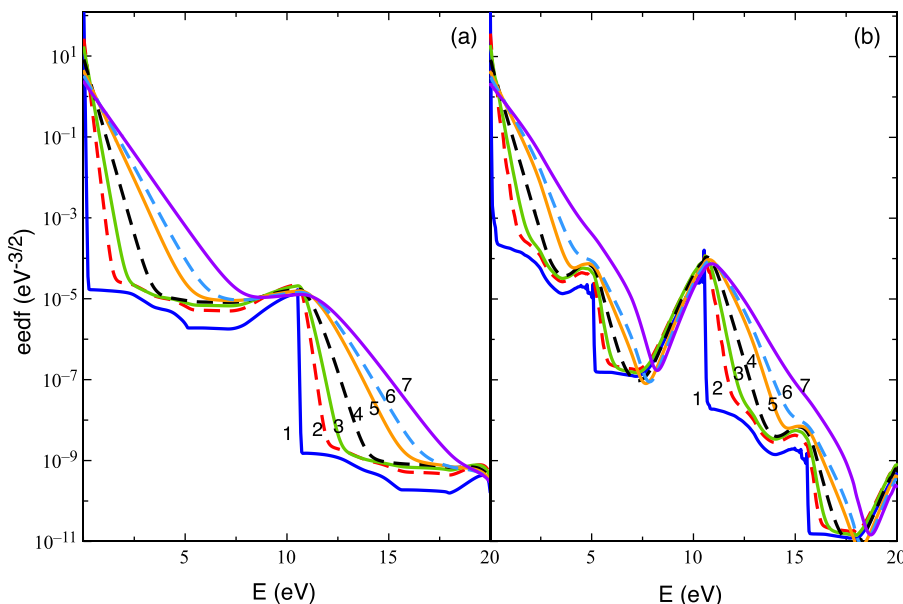
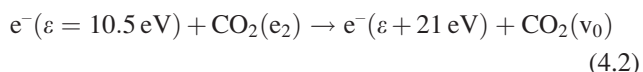


FIG. 6. (a) and (b) Electron energy distribution function versus the electron energy, in the post discharge regime ($E/N=0$ Td), with a concentration of $\text{CO}_2(e_2)$ electronic excited states of 10^{-4} , for different couples of (T_1-T_2) vibrational temperatures (see Table II), (a) including and (b) neglecting e-e collisions (ionization degree of 10^{-3}).



This source of electrons is then spread for $0 < \varepsilon < 10.5 \text{ eV}$ through inelastic and elastic collisions. On the other hand, a new source of electrons is generated at 21 eV through the process



which, similarly, is spread in the energy range 10.5–21 eV through inelastic and elastic collisions, generating the structures reported in Fig. 6(b). These structures are largely smoothed by e-e collisions as reported in Fig. 6(a), dramatically affecting the behavior of eEdf. In particular, in the low vibrational temperature cases, e-e collisions exalt the structures created by superelastic electronic collisions creating a long plateau extending from 10.5 eV to the intersection of the plateau with the low temperature Maxwell distribution, describing the low energy portion of eEdf with $T_e = T_2$, i.e.,

there is a strong coupling between the superimposed vibrational temperature and electron temperature (see, for example, Ref. 27). The increase of vibrational temperature tends to eliminate the corresponding structures, a behavior which can be reproduced with the golden rule reported in Ref. 28. It should be noted that low energy part of eEdf of curve 1 of Fig. 6(a), i.e., the case with $T_1 = T_2 = 0$, can be represented by a Maxwell distribution at $T_e = T_{\text{gas}} = 500 \text{ K}$. In the absence of the electronically excited states, i.e., in the absence of the plateau, this distribution will persist in all the energy range.

It can be noted that curves 1–2 of Fig. 6(b) can reproduce the vibrational situation of a DBD discharge in Kozak *et al.*⁴

It is interesting to follow the time evolution of eEdf from the initial condition determined by the residence time in the discharge up to the achievement of the stationary condition.

Figs. 7(a) and 7(b) report this temporal trend in the presence and absence of e-e collisions taking as initial

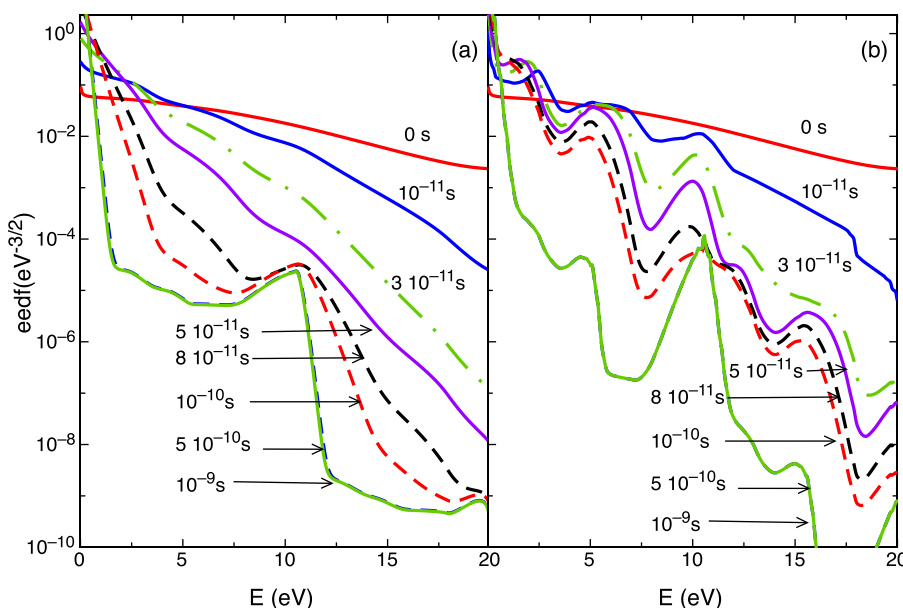


FIG. 7. (a) and (b) Time dependent electron energy distribution function, in the post discharge ($E/N=0$ Td), (a) including and (b) neglecting e-e collisions, for $T_1 = 500 \text{ K}$ and $T_2 = 1500 \text{ K}$ (case 2 of Table II) (ionization degree of 10^{-3} , concentration of $\text{CO}_2(e_2)$ electronic excited state of 10^{-4} , pressure of 1 atm).

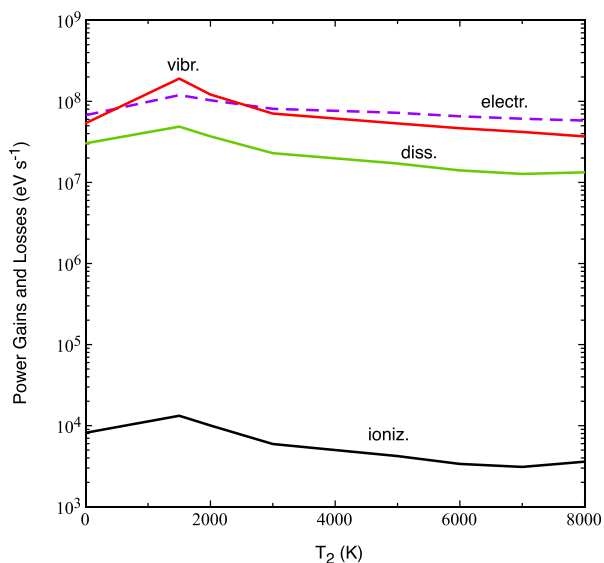


FIG. 8. Electron energy power gains (dashed lines) and losses (solid lines) for vibrational, dissociation, electronic excitation, and ionization channels, in the post discharge regime ($E/N=0$ Td), including e-e collisions (ionization degree of 10^{-3} , concentration of $\text{CO}_2(e_2)$ electronic excited state of 10^{-4}).

condition a well-developed eedf with a concentration of the 10.5 eV electronic state equal to 10^{-4} and small concentration of vibrational excited states ($T_1=500$ K and $T_2=1500$ K). All the stationary results reported in the previous figures as a function of E/N do not depend on the pressure. On the contrary, the time dependent results of Figs. 7(a) and 7(b) depend on pressure. An atmospheric pressure has been chosen to follow the post discharge behaviour activated by a pulse in the nanosecond scale. In this context, we have selected, as a $t=0$ s condition, the eedf obtained with a pulse of 80 Td and an ionization degree of 10^{-3} , which roughly describes the initial conditions of the post discharge regime.

As we can see, the eedf cools down and only when it is cold enough the peak due to superelastic electronic collisions from the 10.5 eV excited level appears. The presence of e-e

collisions is dominant in all the temporal evolution even though the times to reach quasistationary conditions are the same in the two cases ($t \approx 10^{-9}$ s). These times are important to understand the role of excited states in the post discharge conditions following nanopulsed discharge as well DBD ones.

Fig. 8 reports the electron power losses (full lines) and gains (dashed lines) in post discharge conditions. Note that, in this case, we have reported the energy transferred per unit time (eV s^{-1}) to the different CO_2 excitation channels, in particular, for the vibrational one, the reported quantity is Q_{vib}/N_e (see Eq. (2.6)).

By looking at Fig. 8, we can observe that electrons lose energy towards all channels (vibrational, dissociation, and ionization), gaining energy only from the electronic excitation level. This gain is, in absolute value, higher than the losses due to dissociation and ionization and, with the only exception at lower vibrational temperatures, higher than the total energy exchange with the vibrational modes. This result confirms that, also from an energetic point of view, the electronic excited level e_2 dominates the kinetics in post discharge conditions.

It should be noted that in Fig. 8, basically, the electronic energy net gain balances the vibrational, dissociative, and ionization net losses, the maximum difference is within 10% being due to the numerical method used to calculate energy channels, characterized by an error depending on the used electron energy discretization.

V. INTRODUCTION OF A NEW SET OF E-V CROSS SECTIONS IN THE BOLTZMANN SOLVER

The results presented in Sections II–IV have shown the strong coupling between the eedf and both the vibrational temperatures and the electronically excited state concentration, the latter especially in post discharge regime. In order to develop advanced plasma kinetic models that take into account these couplings, a reformulation of the database of electron-impact collision cross sections is necessary, since the most quoted compilations refer to those developed

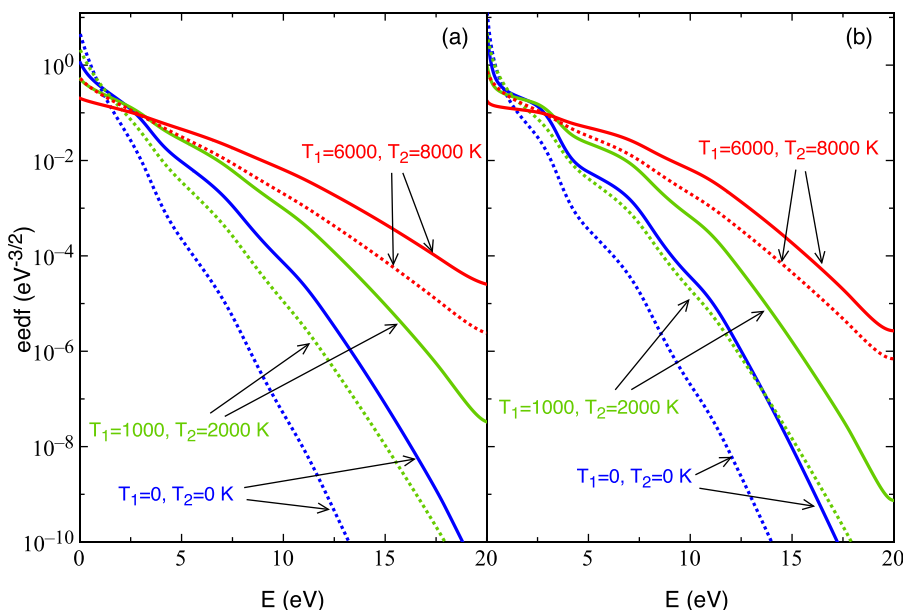


FIG. 9. (a) and (b) Electron energy distribution function versus the electron energy with (dashed lines) and without (full lines) the insertion of more asymmetric levels (00n) up to the dissociation limit in discharge condition ($E/N=30$ Td) (a) with (b) without e-e collisions (ionization degree of 10^{-3}).

by Hake and Phelps,¹⁰ Hayashi,²⁹ and Itikawa,²¹ which, however, refer to the ground state CO₂ molecules. A large effort is therefore necessary to the compilation of a database of electron CO₂ resonant and direct collisions involving vibrationally excited molecules to be used in the development of advanced plasma models.^{30,31} *Ab initio* and phenomenological approaches can be used to this end taking into account the enormous effort made in the literature on electron-diatomic molecule cross sections in the whole vibrational ladder.¹⁴

To better understand this point, in the present section, we show the possible effect of introducing new cross sections in the Hake and Phelps database.¹⁰ In particular, due to the importance of the asymmetric mode in the accepted reaction scheme, we add all e-V cross sections connecting the asymmetric ladder. To this end, we use the semi empirical equation from Fridman,¹¹ as reported by Ref. 4, to obtain the excitation cross sections σ_{nm} for the excitation from $(00v_n)$ to $(00v_m)$ from the known cross section σ_{01}

$$\sigma_{nm}(\varepsilon) = \frac{\exp(-\alpha(m-n-1))}{1 + \beta n} \sigma_{01}(\varepsilon + E_{01} - E_{nm}), \quad (5.1)$$

where $E_{01} = E_1 - E_0$ and $E_{nm} = E_m - E_n$ are the corresponding threshold energies for the excitation and, for CO₂, $\alpha = 0.5$ and $\beta = 0$, as indicated by Ref. 11.

Figs. 9(a) and 9(b) compare eedf with and without the insertion of the new sets of cross sections in discharge conditions for $E/N = 30$ Td and at different vibrational temperatures, showing large differences, partially reduced by the presence of electron-electron collisions.

Fig. 10 shows the same comparison in the post discharge conditions. The insertion of new e-V cross sections does not strongly change the behaviour of eedf in this case, since a large role is taken from the superelastic collision of the 10.5 eV electronically excited state.

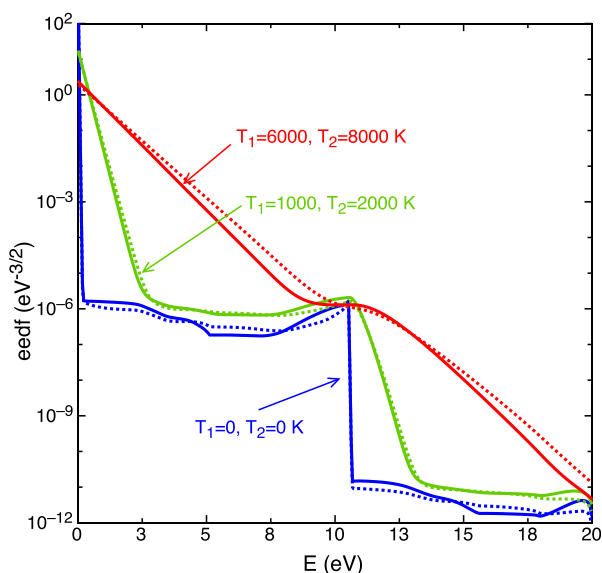


FIG. 10. Electron energy distribution function versus the electron energy with (dashed line) and without (full lines) the insertion of more asymmetric levels $(00n)$ up to the dissociation limit in the post discharge regime.

VI. CONCLUSIONS

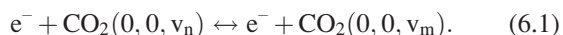
The parametric solution of the electron Boltzmann equation as a function of the vibrational temperatures, the ionization degree, and the electric field values, in CO₂ plasma, has shown the strong coupling between eedf and vibrational and electronically excited state population. As a consequence, the electron fraction power dissipated into the different excitation channels depends strongly on the vibrational excitation, showing that caution occurs in taking as indicator the corresponding results in the cold gas approximation.

By collecting rate data as a function of the average electron energy in discharge and post discharge conditions, we have observed the non-uniqueness of these rates at fixed average electron energy, showing their dependence on non equilibrium plasma conditions. This result occurs especially at low electron average energy and is neglected in global model approach.

It should be again stressed the strong non equilibrium character of eedf in all the reported cases. In particular, in the case of post discharge conditions, one can note that the different eedf (see Figs. 6(a) and 6(b)) are characterized by a quasi-Maxwellian portion in the low energy range followed by a long plateau due to second kind collisions from electronically excited states. The quasi-Maxwellian portion can be characterized by an electron temperature T_e approximately equal to T_2 as a result of the balance between inelastic and superelastic vibrational losses and gains. However, large errors can be done if one uses this electron temperature to calculate the rates of high threshold energy processes, which in the conditions of Figs. 6(a) and 6(b) are controlled by the eedf's plateaux. More in general the results presented in this paper warn the use of Maxwellian distribution functions for eedf (and therefore of T_e). Differences up to several orders of magnitude can be found when comparing high energy threshold rates from correct eedf and the corresponding ones by using Maxwell distribution functions at the same average energy as pointed out by Lj Petrovich *et al.*^{25,26} and confirmed in Figs. 5(a)–5(d).

The present calculations are important to determine the upper limits to the dissociation rates through pure vibrational mechanisms as well as through electron impact direct mechanisms as shown in Ref. 12 and more extensively in Ref. 32.

The accuracy of the present results largely depends on the data input in the Boltzmann solver. The corresponding database, as pointed out in different points of the paper, is that one derived by Hake and Phelps by de-convolution of the experimental swarm transport properties via a Boltzmann analysis. As such, a fair amount of confidence can be attributed to this database when applied to cold gas approximation, i.e., in the absence of large concentrations of excited states. Moreover, the database from swarm de-convolution lacks to a given extent of the uniqueness in the sense that other data sets can reproduce the transport coefficients. Furthermore, the vibrational excitation cross sections considered in the Hake and Phelps data, while rich of coupled mode interaction, do not consider multiquantum transitions along a single mode. We have discussed this problem for transitions in the asymmetric normal mode of CO₂



We can expect a similar behaviour by introducing whole sets of e-V cross sections describing the other two modes of CO₂.

Improvement of the present results can be obtained by a correspondent effort in the atomic and molecular physics describing the electron-CO₂ resonant cross sections entering in the Boltzmann equation. A new database for the vibrationally excited CO₂ system urges to be developed to improve the reliability of the present results. This new database should contain the dependence of electron molecule (resonant and direct) cross sections on the vibrational quantum numbers of CO₂ target. Some experimental data³³ can help the construction of this new database.

Other improvements deal with the coupling of the Boltzmann equation with the corresponding master equations describing the excited state plasma kinetics as well as the ionization-recombination kinetics. To our opinion, the most important point in this effort is to create more realistic vibrational ladders of the CO₂ molecules, developing corresponding databases for both electron molecule and molecule-molecule collisions.

The main results of the present paper, i.e., the large influence of excited states on eedf, should be seriously taken into account in any future development of the CO₂ kinetics in cold plasmas.

ACKNOWLEDGMENTS

This work received funding from the project “Apulia Space,” PON 03PE-00067.6 from DTA Brindisi (Italy).

- ¹M. Capitelli, C. Gorse, M. Berardini, and G. L. Braglia, *Lett. Nuovo Cimento* **31**, 231 (1981).
- ²G. Colonna, M. Capitelli, S. De Benedictis, C. Gorse, and F. Paniccia, *Contrib. Plasma Phys.* **31**, 575 (1991).
- ³M. Kumar, A. Biswas, P. Bhargav, T. Reghu, S. Sahu, J. Pakhare, M. Bhagat, and L. Kukreja, *Opt. Laser Technol.* **52**(0), 57 (2013).
- ⁴T. Kozák and A. Bogaerts, *Plasma Sources Sci. Technol.* **23**, 045004 (2014); **24**, 015024 (2015).
- ⁵R. Aerts, W. Somers, and A. Bogaerts, *ChemSusChem* **8**(4), 702 (2015).
- ⁶T. Silva, N. Britun, T. Godfroid, and R. Snyders, *Plasma Sources Sci. Technol.* **23**, 025009 (2014).
- ⁷A. Fridman, *Plasma Chemistry* (Cambridge University Press, 2012).

- ⁸X. Tao, M. Bai, X. Li, H. Long, S. Shang, Y. Yin, and X. Dai, *Prog. Energy Combust. Sci.* **37**, 113 (2011).
- ⁹W. L. Nighan, *Phys. Rev. A* **2**(5), 1989 (1970).
- ¹⁰R. D. Hake, Jr. and A. V. Phelps, *Phys. Rev.* **158**, 70 (1967); see http://nl.xcat.net/data/set_type.php for Phelps database.
- ¹¹A. Fridman and L. A. Kennedy, *Plasma Physics and Engineering* (CRC press, 2004).
- ¹²L. D. Pietanza, G. Colonna, G. D’Ammando, A. Laricchiuta, and M. Capitelli, *Plasma Sources Sci. Technol. (Fast Track Commun.)* **24**, 042002 (2015).
- ¹³S. D. Rockwood, *Phys. Rev. A* **8**, 2348 (1973).
- ¹⁴N. A. Dyatko, I. Kochetov, and A. Napartovich, *Plasma Phys. Rep.* **28**(11), 965 (2002); *J. Phys. D: Appl. Phys.* **26**(3), 418 (1993); N. A. Dyatko, Y. Z. Ionikh, N. B. Kolokolov, A. V. Meshchanov, and A. P. Napartovich, *IEEE Trans. Plasma Sci.* **31**(4), 553 (2003).
- ¹⁵G. Colonna, C. Gorse, M. Capitelli, R. Winkler, and J. W. Wilhelm, *Chem. Phys. Lett.* **213**, 5 (1993).
- ¹⁶G. Colonna and M. Capitelli, *J. Therm. Heat Transfer* **22**(3), 414 (2008).
- ¹⁷G. D’Ammando, M. Capitelli, F. Esposito, A. Laricchiuta, L. D. Pietanza, and G. Colonna, *Phys. Plasmas* **21**, 093508 (2014).
- ¹⁸M. Capitelli, R. Celiberto, G. Colonna, F. Esposito, C. Gorse, K. Hassouni, A. Laricchiuta, and S. Longo, *Fundamental Aspects of Plasma Chemical Physics, Kinetics*, Spinger Series on Atomic, Optical, and Plasma Physics (Springer, New York, 2016).
- ¹⁹A. D’Angola, G. Coppa, M. Capitelli, C. Gorse, and G. Colonna, *Comput. Phys. Commun.* **181**, 1204 (2010).
- ²⁰R. D. White, R. E. Robson, B. Schmidt, and M. A. Morrison, *J. Phys. D: Appl. Phys.* **36**, 3125 (2003).
- ²¹Y. Itikawa, *J. Phys. Chem. Ref. Data* **31**(3), 749 (2002).
- ²²I. Armenise and E. V. Kustova, *Chem. Phys.* **415**, 269 (2013).
- ²³K. J. Siemsen, J. Reid, and C. Dang, *IEEE J. Quantum Electron.* **16**(6), 668 (1980).
- ²⁴R. Aerts, T. Martens, and A. Bogaerts, *J. Phys. Chem. C* **116**(44), 23257 (2012).
- ²⁵Z. Lj Petrovic, S. Dujko, D. Maric, G. Malovic, Z. Nikitovic, O. Sasic, J. Jovanovic, V. Stojanovic, and M. Radmilovic-Radenovi, *J. Phys. D: Appl. Phys.* **42**, 194002 (2009).
- ²⁶Z. Lj Petrovic, M. Suvakov, Z. Nikitovic, S. Dujko, O. Sasic, J. Jovanovic, G. Malovic, and V. Stojanovic, *Plasma Sources Sci. Technol.* **16**, S1–S12 (2007).
- ²⁷C. Gorse, M. Capitelli, and A. Ricard, *J. Chem. Phys.* **82**, 1900 (1985).
- ²⁸G. D’Ammando, G. Colonna, M. Capitelli, and A. Laricchiuta, *Phys. Plasmas* **22**, 034501 (2015).
- ²⁹M. Hayashi, in *Non-equilibrium Processes in Partially Ionized Gases*, edited by M. Capitelli and J. N. Bardsley (Plenum Press, New York, 1990).
- ³⁰G. Colonna, V. Laporta, R. Celiberto, M. Capitelli, and J. Tennyson, *Plasma Sources Sci. Technol.* **24**, 035004 (2015).
- ³¹M. Capitelli, G. Colonna, G. D’Ammando, V. Laporta, and A. Laricchiuta, *Phys. Plasmas* **20**(10), 101609 (2013).
- ³²L. D. Pietanza, G. Colonna, G. D’Ammando, A. Laricchiuta, and M. Capitelli, “Non equilibrium vibrational assisted dissociation and ionization mechanisms in cold CO₂ plasmas,” *Chem. Phys.* (submitted).
- ³³S. J. Buckman, M. T. Elford, and D. S. Newman, *J. Phys. B* **20**, 5175 (1987).